Spinodal Fluctuations of Budding Vesicles

Hans-Günther Döbereiner,[1,2,3] Evan Evans,[2] Udo Seifert,[3] and Michael Wortis[1]

[1]*Physics Department, Simon Fraser University, Burnaby, British Columbia, Canada V5A 1S6*

[2]*Department of Physics, University of British Columbia, 6224 Agriculture Road, Vancouver, British Columbia, Canada V6T 2A6*

[3]*Max-Planck-Institut für Kolloid- und Grenzflächenforschung, Kantstrasse 55, 14513 Teltow-Seehof, Germany*

(Received 15 May 1995)

We report the first systematic observations of precursor effects in shape transitions of phospholipid-bilayer vesicles in aqueous solution. Vesicles change abruptly, as temperature T is raised, from a prolate ellipsoidal shape to a "budded" shape consisting of two unequal spheres connected by a narrow neck. On the low-T side of this transition, we see large thermal shape fluctuations (quasicritical fluctuations) and long relaxation times (quasicritical slowing down), which may be interpreted, in the context of a ϕ^6 Landau theory, as the fluctuations of a metastable state near its spinodal instability.

PACS numbers: 82.70.–y, 05.40.+j, 68.10.–m

Fluid-phase phospholipid-bilayer vesicles in aqueous solution exhibit a variety of shapes [1–5]. As vesicle parameters such as area A and volume V are smoothly varied (e.g., by controlling the ambient temperature), these shapes evolve in an analytic manner except at special boundaries. At these "shape transitions," changes in shape are either discontinuous (first order) or continuous but with a change of symmetry class (second order). Hysteresis occurs at first-order transitions, whenever (as is common) energy barriers are larger than thermal energies. Even though thermal fluctuations ("flickering" [6]) of vesicle shape are commonly observed, bending-elastic energies are typically appreciably larger than room temperature, so that mean shapes are reasonably well defined. Likewise, distinct symmetry classes of shapes are normally readily identifiable. Here, we will focus on the "budding" transition, at which an up-down symmetric prolate ellipse transforms, as T is increased, to a shape consisting of two asymmetric spheres joined at a narrow neck. This transition was studied earlier for DMPC vesicles [2] and was interpreted as a second-order symmetry-breaking transition from the ellipse to a pear shape, followed by a first-order transition to the final budded configuration, a sequence inconsistent with extant theories [4,5]. We now believe [4] that budding is a hysteretic effect associated with a spinodal instability. We report in this Letter large-amplitude long-time fluctuations near the budding threshold, which we interpret as the spinodal analog (at the mean-field level) of thermodynamic critical behavior. This is the first time that such "quasicritical" behavior has been documented for a vesicular instability.

We report experiments on SOPC vesicles in which the thermally induced shape fluctuations were dynamically imaged via phase-contrast video microscopy at a sequence of temperatures approaching the transition temperature from below. By parametrizing the projected vesicle-shape contours in terms of Fourier-mode amplitudes, we were able to monitor quantitatively both the static shape fluctuations and the time-dependent mode-mode correlation functions. We observed an ensemble of shapes that preserves (to a good approximation) the up-down symmetry of the ellipsoidal branch, not in the sense that each individual shape has this symmetry but in the sense that for each "up" fluctuation there is an equivalent "down" fluctuation somewhere in the time sequence; see Fig. 1. Our analysis focuses on the lowest mode that breaks the up-down symmetry. Approaching the transition, we document a striking growth in both the static fluctuations of this mode and its dominant (overdamped) relaxation time. Both these quantities appear to exhibit power-law behavior in an interval near the transition.

It is believed that the dependence of the energy E of a phospholipid-bilayer vesicle on its shape S is described at the mesoscopic level by a functional [4,7,8]

$$E[S] = \frac{\kappa}{2} \oint dA[C_1 + C_2 - C_0]^2 + \frac{\bar{\kappa}}{2} (m[S] - m_0)^2. \tag{1}$$

Here, $C_1(\mathbf{r})$ and $C_2(\mathbf{r})$ are the two principal curvatures at the point $\mathbf{r}$ of the vesicle surface; C_0 is the spontaneous curvature; κ is the bending rigidity; and the integral is over the entire vesicle surface. In the second term, $\bar{\kappa}$ is the nonlocal bending modulus, and $m[S] \equiv \oint dA(C_1 + C_1)/2R_A$ measures the area difference between the two leaves of the bilayer in a way that has been made dimensionless by dividing out the area length scale R_A ($A \equiv 4\pi R_A^2$). This term measures the elastic energy cost of forcing the actual area difference to differ from its "relaxed" value (mea-

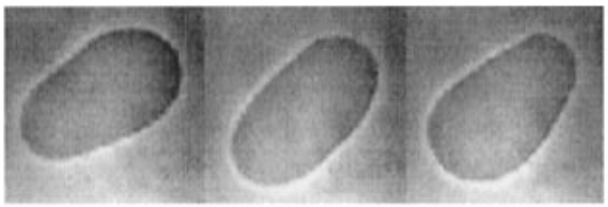

FIG. 1. Snapshots of pear fluctuations of a prolate vesicle at reduced volume $v = 0.912$.

 0031-9007/95/75(18)/3360(4)$06.00

sured by m_0), which reflects the different number of lipid molecules in the two leaves. The ratio $\alpha \equiv \bar{\kappa}/\kappa$ is of order unity ($\alpha \sim 1.4$ for SOPC [4,9]). The overall area and volume may be regarded as fixed. The whole problem can be expressed in terms of the energy scale $\kappa \sim 25 k_B T_{\text{room}}$ (SOPC [9]) and the dimensionless parameters, α, $v \equiv 3V/4\pi R_A^3$ (reduced volume), $c_0 = C_0 R_A$ (reduced spontaneous curvature), and m_0, of which the last three are individually specific to each vesicle.

Variation of Eq. (1) with respect to the shape S leads to a discrete set $\{n\}$ of stationary shapes $S_n(v, m_0, c_0, \alpha)$ with corresponding energies $E_n(v, m_0, c_0, \alpha)$ for each set of control parameters. The energies E_n vary smoothly as functions of the control parameters, except at special singular points. Only the lowest-energy shape is thermodynamically stable; however, other low-lying locally stable shapes are often seen in the laboratory. The control parameters vary with temperature, so, as T is raised, each vesicle follows some trajectory through the parameter space (v, m_0, c_0, α). Thus, a prolate shape that is the lowest energy at low laboratory temperature may become metastable as T increases, when the prolate branch crosses the pear branch. Now, Eq. (1) shows that energy barriers are generically of order κ ($\gg k_B T$); thus, metastability will continue beyond the level-crossing temperature, until the energy barrier to escape from the local prolate minimum becomes comparable to $k_B T$. Gaussian fluctuations about the metastable shape scale as $k_B T/\epsilon$, where ϵ is a typical normal-mode energy, generically of order κ. As the limit of metastability is approached, one (or more) of the modes becomes soft, signaling the onset of the instability (bifurcation). We argue that this soft-mode mechanism is responsible for the large, slow fluctuations near the budding transition. We give below a Landau theory description of this bifurcation.

Bilayer vesicles of SOPC were prepared [5] by swelling dry lipid in 50 mMol sucrose solution and then suspending in excess 48 mMol glucose solution, adjusted so that the overall density of the vesicles was slightly greater than that of the surrounding aqueous solution. Thus, vesicles rested against the bottom of the observation chamber, where they were observed from below via video phase-contrast microscopy. With appropriate preparation and vesicle selection [10], the target vesicle rested gently enough against the bottom so that its shape was not detectably deformed yet strongly enough so that full rotational diffusion of the vesicle was inhibited. Thus, a vesicle of prolate elliptical shape had its symmetry axis restricted effectively to the horizontal plane. The video camera, focused on the axial plane, recorded an image every 1/30 sec.

A two-dimensional outline of the vesicle was prepared for each grabbed frame by a protocol that scans the grey scale pixel by pixel across the halo and locates a nominal membrane point where the grey-scale profile crosses its local background level. Finally, a local smoothing algorithm [5] was applied to these outline points in order to reduce noise. A frame was grabbed every 0.5 sec and processed in real time. At least 1200 images were processed for each temperature to establish an ensemble. Each data set took about 20 min to accumulate, including temperature ramping and equilibration.

In these experiments, the vesicle shape was approximately prolate elliptical. We located a nominal principal axis by treating the contour as a uniform line density and calculating the axes of the corresponding inertia tensor. We then parametrized the shape of each half contour in terms of an arclength s measured from one pole (the pole-to-pole arc length is s^*) and the angle ψ between the normal to the axis and the local tangent to the contour at s. It is convenient to describe each half contour via the scale-independent Fourier representation

$$\psi(s) = \pi s/s^* + \sum_{n=1} a_n \sin[n(s/s^*)\pi]. \qquad (2)$$

The linear term describes a half circle. Nonzero coefficients $\{a_n\}$ describe deviations from the circle. Up-down symmetric shapes obey $a_{2n+1} = 0$ for all n.

The information in each "snapshot" was coded in a set of shape amplitudes $\{a_n\}$. Using the data for a single vesicle observed over a long period of time [11], we then constructed ensemble averages like $\langle a_n \rangle$, $C_n \equiv \langle \Delta a_n^2 \rangle$, where $\Delta a_n \equiv a_n - \langle a_n \rangle$, and so forth. Likewise, we formed time-dependent mode-amplitude correlations like $C_n(t) \equiv \langle \Delta a_n(t + t') \Delta a_n(t') \rangle$, which depend only on the time difference t for a stationary ensemble.

Deep in the prolate phase, away from the budding instability, the mean amplitudes $\langle a_n \rangle$ are well defined and decrease rapidly with n [12]. Thus, for the particular vesicle [11], which we shall study in detail below, we found, e.g., at $v = 0.931 \pm 0.002$, that $\langle a_2 \rangle \simeq 0.37$, $\langle a_4 \rangle \simeq 0.04$, $\langle a_6 \rangle \simeq 0.001$, and $\langle a_{2n+1} \rangle \leq 0.001$. In this region, fluctuations were small, and we estimated the reduced volume [5] v by rotating each instantaneous contour about its symmetry axis, calculating the enclosed volume, and averaging over the ensemble. Figure 2 shows the mean-square amplitude fluctuations, C_n, $n = 1$–6, in their dependence on reduced volume. Note that for even n the fluctuations are only weakly volume dependent. By contrast, the $n = 3$ fluctuations (and at a less visible level those for $n = 1$ [13]) grow significantly as the reduced volume approaches the point [14], $v_b = 0.878 \pm 0.004$, at which budding occurs. In fact, the $n = 3$ mode is the lowest-lying mode that breaks the up-down symmetry of the prolate shape. Figure 3 shows directly the growth of the $n = 3$ fluctuations as a function of reduced volume. A power-law fit of the form

$$C_3 \sim A_3/(v - v_b)^{\gamma_s} \qquad (3)$$

suggests an exponent for the static fluctuations of $\gamma_s = 0.83^{+0.21}_{-0.17}$, the significance of which will become apparent below.

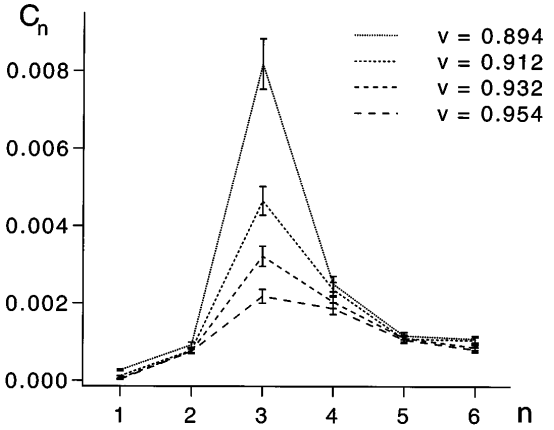

FIG. 2. Mean-square amplitudes (C_3) at four different reduced volumes approaching budding. Note the strong growth of the mode a_3 and the relative constancy of the even modes. Uncertainties are shown; the lines are guides for the eye.

The time-dependent correlations $C_n(t)$ typically decayed monotonically. It was convenient to fit this decay to an exponential [15], $C_n(t) \sim B_n \exp(-t/\tau_n)$, and, thus, to define a characteristic dominant relaxation time τ_n for each mode n. Well away from the budding instability, the relaxation times were 1–2 sec for the low modes, $n = 1, 2, 3, 4$, and shorter for higher modes. However, the relaxation time for the $n = 3$ mode increased significantly as the budding instability was approached. This increase, shown in Fig. 3, was obvious in the video pictures, where we observed large, slow pearlike fluctuations about the elliptical average shape, first to one side and then to the other; see Fig. 1. A crude fit of the power-law type gave $\tau_3 \sim D_3/(v - v_b)^{\gamma_d}$ with a dynamical exponent γ_d of order 1 but with large uncertainty.

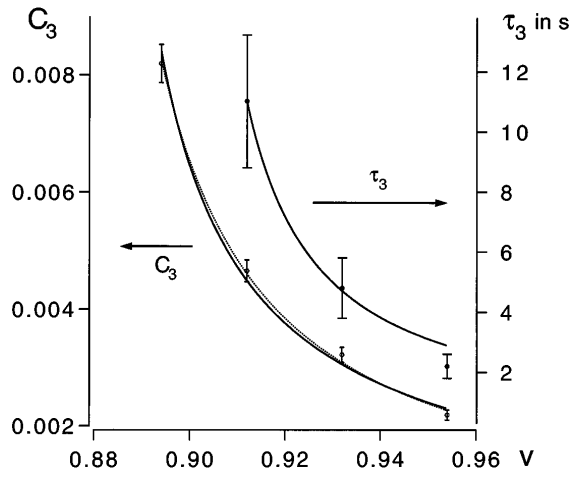

FIG. 3. Growth of static fluctuations (C_3) in the mode a_3 and the corresponding dominant relaxation time (τ_3). Both quantities increase strongly near budding. For C_3, the full curve shows a two-parameter fit by Eq. (3) with the experimental v_b, giving γ_s as quoted in the text; the dotted curve forces $\gamma_s = 1$ and finds $v_b = 0.871 \pm 0.003$. Likewise the curve for τ_3 shows a fit with $\gamma_d = 1$ and gives $v_b = 0.897 \pm 0.005$.

There is a simple interpretation of these observations. For the values of m_0 of relevance here, the (up-down symmetric) prolate is the lowest-energy shape for high reduced volumes, $v \simeq 1$. As laboratory temperature T is increased, thus decreasing the value of v, the system first enters a metastable regime where the lowest-energy shape is pearlike but the prolates remain stable against local fluctuations [4]. Later, at a reduced volume v_b, the prolates become locally unstable to a pear mode, which eventually carries them over an energy barrier and down to the asymmetric minimum-energy shape, which is budded. At the Landau-theory level, we may characterize this sequence of events by an energy functional

$$V(a) = \kappa[\tfrac{1}{2}ra^2 - \tfrac{1}{4}ga^4 + \tfrac{1}{6}ua^6], \qquad (4)$$

where κ sets the overall energy scale, a is the amplitude of the mode that becomes soft at v_b, and the remaining parameters, r, $g > 0$, and $u > 0$, are dimensionless. The symmetrical (prolate) branch is metastable in the range $0 < r < 3g^2/16u$; the limit of metastability occurs as $(v - v_b) \sim r \to 0^+$. The unstable mode can, in principle, be a mixture of all the odd modes $\{a_n\}$. In practice, the data suggest that a_3 tends to dominate. We will use the description Eq. (4) only near the prolate state ($a \sim 0$). There is no suggestion that the eventual budded shape should be described by a single amplitude.

Static thermal fluctuations of the metastable prolate shape are controlled by the part of the energy landscape inside the metastability barrier, which for r small is located close to $a^2 = r/g$ with height $\kappa r^2/4g$. Amplitude fluctuations are given at the Gaussian level by $\langle a^2 \rangle = k_B T/\kappa r$, which is only expected to be valid when $\langle a^2 \rangle \ll r/g$, so the non-Gaussian terms may be neglected. Indeed, when this criterion is not satisfied, there is significant probability of escape over the barrier. It follows that there is a range of reduced volume, $gk_B T/\kappa \ll r^2 \ll 1$, near but not too near the budding instability, for which the static fluctuations are predicted to grow as $(v - v_b)^{-1}$, as is consistent with the observations, Eq. (3).

Discussion of the time dependence of the modes requires a dynamical theory, which must in general contain information about solvent properties [16]. For present the purposes we shall simply assume that the soft mode obeys a dynamical equation of the purely dissipative type,

$$\partial a/\partial t = -\Gamma \partial V/\partial a + \zeta, \qquad (5)$$

where ζ is the usual noise term. Equation (5) simplifies to $\partial a/\partial t = -\Gamma \kappa r a + \zeta$ near $a = 0$, when the Gaussian term dominates. The kinetic coefficient Γ has dimension such that $\Gamma^{-1} \sim$ time $\times$ energy. The dominant mechanism for dissipation is via the solvent viscosity η; the appropriate length scale for the unstable mode is the size scale R of the vesicle. Thus, dimensional analysis leads to $\Gamma = c/\eta R^3$, with a numerical factor c that is generically

of order unity. In the regime described above, where the Gaussian term dominates V, Eq. (5) predicts

$$\langle a(t)a(0)\rangle = \langle a^2\rangle e^{-t/\tau}, \tag{6}$$

with $\tau = (\Gamma\kappa r)^{-1} \sim (v - v_b)^{-1}$, which is consistent with the observations. Furthermore, inserting typical parameter values, $\eta = 10^{-2}$ erg sec/cm^3, $R = 10^{-3}$ cm, and $\kappa = 10^{-12}$ erg, we estimate the typical (slowest) relaxation time as $t \sim 10/(v - v_b)$ sec, in good agreement with the observations.

The Landau picture of the observed pretransitional behavior suggests for the "spinodal exponents" $\gamma_s = \gamma_d = 1$. We now understand that these "power laws" are at best valid near but not too near the instability. Nevertheless, if we accept these values, we can reanalyze the data displayed in Fig. 3, treating the position of the spinodal v_b as unknown. This procedure leads to estimates $v_b = 0.871 \pm 0.003$ from the static data and $v_b = 0.90 \pm 0.01$ from the relaxation-time data, in reasonable agreement with the observed point of budding.

In the theory of phase transitions, a boundary that describes the limit of stability of a metastable state or phase (at the mean-field level) is referred to as a "spinodal." Behavior near such a spinodal is in some ways analogous to behavior near a second-order phase transition [17]. In a true thermodynamic second-order transition, both the characteristic fluctuation amplitude and the dominant relaxation time ultimately diverge at the transition but with exponents renormalized from their mean-field values by cooperative effects due to the many long-wavelength degrees of freedom. For a spinodal, on the other hand, this divergence is never achieved because the fluctuating state is globally unstable and decays when the fluctuations reach a finite size. For a simple mechanical system like the vesicle, there is only one unstable mode, so no renormalization occurs.

This kind of mechanical instability produced by mode softening is not uncommon. What is unusual is to have a system in which the energy barrier in the metastable state is only a few times k_BT, so that significant pretransitional fluctuations can occur, and in which the height of the barrier can be controlled delicately on the scale of k_BT (as is done here by controlling the temperature), so that these fluctuations can be accessed and explored in a systematic manner.

We are grateful for discussions with W. Rawicz, A. Leung, M. Nikolić, J. Käs, and E. Sackmann. M. W. is grateful for the hopitality of the Max-Planck-Institut für Kolloid- und Grenzflächenforschung, where this manuscript was written. This work was supported in part by a Natural Sciences and Engineering Research Council of Canada grant (M. W.) and a Medical Research Council of Canada grant (E. E.).

[1] K. Berndl, J. Käs, R. Lipowsky, E. Sackmann, and U. Seifert, Europhys. Lett. **13**, 659 (1990).
[2] J. Käs and E. Sackmann, Biophys. J. **60**, 825 (1991).
[3] R. Lipowsky, Nature (London) **349**, 475 (1991).
[4] L. Miao, U. Seifert, M. Wortis, and H.-G. Döbereiner, Phys. Rev. E **49**, 5389 (1994), and references therein.
[5] H.-G. Döbereiner, Ph.D. thesis, Simon Fraser University, 1995 (unpublished).
[6] M. B. Schneider, J. T. Jenkins, and W. W. Webb, J. Phys. (Paris) **45**, 1457 (1984); H. Engelhardt, H. Duwe, and E. Sackmann, J. Phys. Lett. **46**, L395 (1985).
[7] W. Helfrich, Z. Naturforsch. **28c**, 693 (1973); E. Evans, Biophys. J. **14**, 923 (1974); **30**, 265 (1980).
[8] S. Svetina, M. Brumen, and B. Žekš, Stud. Biophys. **110**, 177 (1985).
[9] E. Evans and D. Needham, J. Phys. Chem. **91**, 4219 (1987).
[10] The gravitational effect is measured by the dimensionless combination $gR^4\Delta\rho/\kappa$, where g is the gravitational acceleration, R is a typical vesicle dimension, and $\Delta\rho$ is the density difference. Vesicles that are too small rotate freely, while those that are too large are flattened against the bottom of the experimental cell. See Ref. [5] and M. Kraus, U. Seifert, and R. Lipowsky (to be published).
[11] The data that follow are for one of the several vesicles we studied in this manner. Data for the others were similar but are not directly comparable, since m_0 is not a variable that can be selected in the laboratory. Practical difficulties limit accumulation of more extensive data sets: (a) It is hard at this stage to predict when (or even whether) a single vesicle chosen for observation will bud; (b) although thermal trajectories that do not bud are reversible (at least, on time scales that are not too long), the transition in and out of the budded state is always to some extent irreversible, presumably because of the strong short-range forces that come into play when the neck closes down to molecular dimensions; and (c) significant lipid degradation seems to occur on a scale of ca. 6 h.
[12] This behavior is generic for $v \simeq 1$. See Refs. [4] and [5].
[13] For $v \sim 1$, it is easy to show [5] that $a_1 \sim \langle a_2\rangle a_3$, so that a_1 remains small and tracks a_3.
[14] This experimental value of v_b is obtained from the observed temperature of budding ($T_b = 45.8 \pm 0.2$ °C) by extrapolating the decrease of v due to the thermal expansion of the vesicle along its budding trajectory. Vesicle fluctuations were recorded at $T = 28.7$, 32.7, 37.8, and 42.4 °C.
[15] Near the instability, it was necessary to fit by a sum of two exponentials in order to pick up additional, shorter relaxation times.
[16] S. T. Milner and S. A. Safran, Phys. Rev. A **36**, 4371 (1987); U. Seifert and S. A. Langer, Europhys. Lett. **23**, 71 (1993); T. M. Fischer, Phys. Rev. E **50**, 4156 (1994).
[17] At this Gaussian level, pretransitional behavior at a spinodal does not differ from that at a second-order transition. What distinguishes the spinodal is the unstable behavior beyond the transition.